Thermo-Mechanical Material Modelling for Cyclic Loading a Generalized Modelling Approach to Different Material Classes

Holger Sparr(✉), Daniela Schob, and Matthias Ziegenhorn

BTU Cottbus-Senftenberg, Universitätsplatz 1, 01968 Senftenberg, Germany
holger.sparr@b-tu.de

Abstract. The paper presents a modelling approach for thermo-mechanically coupled problems and an experimental concept for a material law validation. The approach is generally applicable to a variety of material classes. The main objective is to integrate viscoplasticity as one major aspect in cyclic loading of high-performance polymers at small deformation gradients. After a classification of the subject a brief outline of the theoretical framework is given, which is then followed by the description of the experimental setup and some specifics to be accounted for. The Paper continues with some results of the numerical analysis on how to validate the applied material law.

1 Introduction

A general task for engineers is to assess the fatigue behaviour of a high perform-ance structural component. The most common load is in fact time-dependent. Therefore fatigue is the cause of 60–80% of all component failures. The com-plexity in terms of low- and high-cycle fatigue incorporating viscoplasticity in the description of classical design materials has been widely studied [1] and is nowa-days transferred to new and more complex material classes like heterogeneous material or additive manufactured plastics.

The mechanical properties of (reinforced) plastics in conventional or additive manufacturing are dominated by the properties of the matrix material. These materials similar to conventional design materials at elevated temperatures exhibit a rate-dependent behaviour and furthermore an equilibrium hysteresis when subjected to a relaxation process on the load path. Additionally, by extending the measurement procedure to cover the temperature field in a cyclic load setting (with a common stress amplitude, mean stress and frequency) we observe a characteristic temperature evolution. The observation of equilibrium hysteresis classifies the material as viscoplastic [2] whereas a significant temperature evolution leads the material modelling to a thermo-mechanical analysis.

To cover the different micro-mechanical phenomena the applied material models and the experimental procedures to establish the set of material parameters need to be adapted. Additionally through the application of thermography, the consideration of an evolving temperature field opens an opportunity to verify the chosen modelling approach and creates further possibilities for proof.

E. Rusiński and D. Pietrusiak (Eds.): CAE 2018, LNME, pp. 705–711, 2019.
https://doi.org/10.1007/978-3-030-04975-1_81

The fully coupled thermo-mechanical model is based on the quantitative evaluation of the second law of thermodynamics. In terms of small deformation gradients for uniaxial loaded specimens the outline of rheological networks offers a comprehensive access [3]. Therefore, the contribution presents a concepts for a suitable material characterization of classical design materials and plastics exploiting different ways of covering viscoplasticity.

A classical continuum mechanical framework with the concept of inner variables was applied in [4]. Here he main focus lies in the hygro-mechanical formulation.

2 Fundamental Equations

The complete formulation is based on the concepts of continuum mechanics. First of all can be named the balance equations (balance of momentum, balance of energy, balance of entropy and conservation of mass) which need to be fulfilled.

In thermo-mechanical analyses with the fundamental coupling of the temperature and displacement field the second law of thermodynamics becomes important and leads to a common result as in (1).

$$\delta = \frac{1}{\varrho}\sigma\dot{\varepsilon} - \dot{e} + \theta\dot{s} - \frac{1}{\varrho\theta}q\frac{\partial\theta}{\partial x} \geq 0 \tag{1}$$

The symbols refer to the internal dissipation δ, the density ϱ, the stress σ, the strain ε, the Helmholtz free energy e, the temperature θ, the entropy s and the heat flux q. The derivative of θ is the temperature gradient.

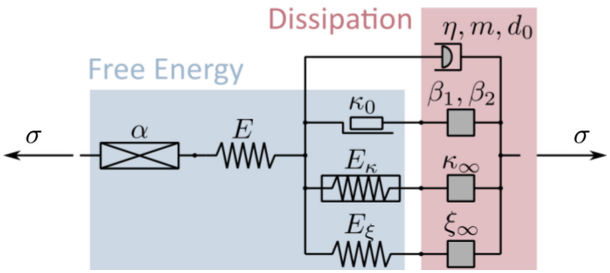

Fig. 1. Simple rheological network as proposed in [3]

The advantage of rheological networks is a straight forward application of additive decomposition rule. The network outlined in Fig. 1 was developed by Broecker et al. [3] and serves as the basis for all further numerical results presented here. The first to chain members combine thermoelasticity as the branched member describes the viscoplasticity. All elements contributing to internal dissipation are highlighted by the red box and are located in the viscoplastic branch. Two of the fundamental additive decompositions for the Helmholtz free energy and the strain are given by Eqs. (2) and (3).

$$e = e_{\text{th}} + e_{\text{el}} + e_{\text{iso}} + e_{\text{kin}} + \ldots \tag{2}$$

$$\varepsilon = \varepsilon_{\text{el}} + \varepsilon_{\text{th}} + \varepsilon_{\text{vp}} \tag{3}$$

The introduction of the material laws, common laws in the sense of elasticity or thermal expansion and non-linear laws based on experimental observations for the viscoplastic and hardening behaviour, lead to set of equation summarized in Table 1.

Table 1. Set of equations

Elastic stress - strain relationship	$\sigma = E\varepsilon_{\text{el}} = E(\varepsilon - \varepsilon_{\text{vp}})$	(4)
Closure of the elastic domain	$\mathbb{E}_\sigma := \{(\sigma, \xi) \in \mathbb{R} \times \mathbb{R} \mid f(\sigma, \xi) \leq 0\}$ with $f(\sigma, \xi) = \lvert\sigma - \xi\rvert$	(5)
Flow rule	$\dot{\varepsilon}_{\text{vp}} = \frac{1}{\eta}\left\langle \frac{f}{d_0} \right\rangle^m \operatorname{sgn}(\sigma - \xi)$ $\dot{\xi} = E_\xi\left(\dot{\varepsilon}_{\text{vp}} - \frac{\xi}{\xi_\infty}\dot{\bar{\varepsilon}}_{\text{vp}}\right)$ with $\dot{\bar{\varepsilon}}_{\text{vp}} = \lvert\dot{\varepsilon}_{\text{vp}}\rvert$	(6)
Thermal expansion	$\dot{\varepsilon}_{\text{th}} = \alpha\dot{\theta}$	(7)
Heat conduction	$c_{\text{def}}\dot{\theta} = -\frac{1}{\rho}E\alpha\theta\dot{\varepsilon}_{\text{el}} + \delta_{\text{M}}$ $\delta_{\text{M}} = \frac{1}{\rho}[f + \frac{\xi^2}{\xi_\infty}]\dot{\bar{\varepsilon}}_{\text{vp}} \geq 0$	(8)

The numerical solution for the evolutionary equations of the one-dimensional problem is set up by a Backward-Euler scheme. The subsequent calculation are carried out by assuming adiabatic boundary conditions.

3 Measurement Procedure

Additional to the classical measurement equipment for mechanical tests on a uni-axial servo-hydraulic testing machine, a temperature sensor is necessary to cover the temperature field evolution. To meet the required accuracy a high-precision IR camera was applied to preliminary tests and proofed applicably (see Fig. 2). The conventional application of IR cameras provide a precision of approximately 20 mK. In terms of cyclic loading at a small deformation gradient it is expected that the temperature evolve at small rates with less than the mentioned standard accuracy in temperature change per cycle. Therefore the Lock-In thermography is going to be applied, where well defined strain or forced controlled load spectra serve as an internal excitations. By transformation of time signal into the frequency domain the precision of measurement can be improved up to 1 mK for a pure elastic deformation process.

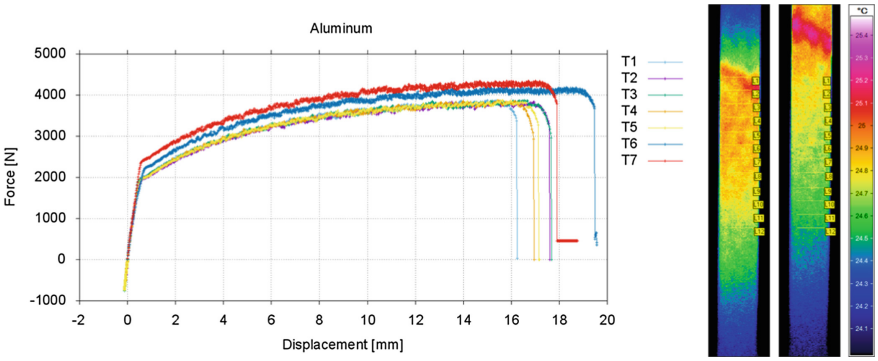

Fig. 2. Tension test and corresponding temperature evolution

The transition in a viscoplastic setting goes beyond the regular usage of Lock-In thermography since the amplitude as well as the phase angle in the frequency domain might be influenced by viscoplastic phenomena, which was already discussed in [5]. The localized effects of (visco-)plastic deformations depicted on the right of Fig. 2. need to be predicted in the test preparation or quantified and assessed as post-test procedure by analytical tools.

A deeper understanding of predicted temperature field gives the opportunity to calibrate the Lock-In measurement for non-standard observation tasks. The experimental observations of energetic physical measures and the correlation to dissipative phenomena in the material points into the very accurate temperature field measurement. In contrast to the Lock-In technology an experimentally complex setup was suggested in [6].

4 Numerical Results

The results presented in this study are based on the material parameters collected in Table 2.

Table 2. Material parameters

Parameter	Unit	Value
Thermo-Elasticity		
Modulus of Elasticity E	N mm^{-2}	60800
Density ϱ	kg/m^3	2900.0
Expansion Coefficient α	K^{-1}	$21,5 \cdot 10^{-6}$
Heat Capacity c_{def}	J/(kg K)	940.0
Thermal conductivity k	W/(m K)	210.0
Friction Element (Dissipation)		
Yield Stress k_0	N mm^{-2}	60
Lin. Dissipation Coeff. β_1	[−]	0…1
Non-lin. Dissipation Coeff. β_2	[−]	0…1

(*continued*)

Table 2. (*continued*)

Parameter	Unit	Value
Kinematic Hardening		
Kin. Hardening Modulus E_k	N mm^{-2}	5250
Kin. Saturation k^{∞}	N mm^{-2}	61.8
Isotrope Verfestigung		
Iso. Hardening Modulus E_{ξ}	N mm^{-2}	5250
Iso. Saturation ξ^{∞}	N mm^{-2}	61.8
Viscosity		
viscosity η	s	1…1000
Viscosity Exponent m	[−]	0.2…5

These parameters can be obtained by fitting experimental data of standard mechanical tests at different strain rates and standard caloric tests. Difficulties can arise in the unique identification of the hardening parameters the since isotropic and kinematic hardening phenomena is addressed simultaneously. A sophisticated verification and validation process needs to established, what can be achieved by applying the described analytical tool to characteristic cycle sequence.

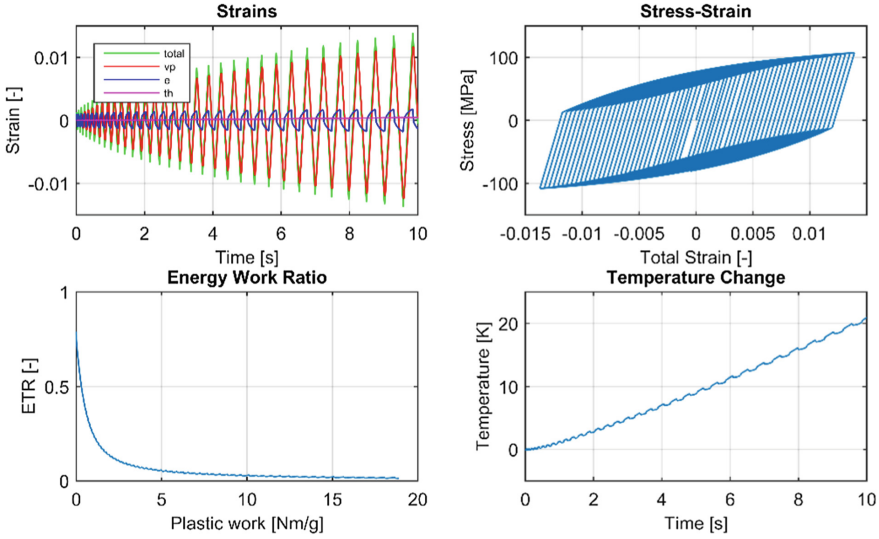

Fig. 3. Cyclic test with a linearly increasing amplitude in tension and compression

An academic strain-controlled cycle sequence is shown in Fig. 3. Since the period of the positive resp. negative strain maxima is constant, the strain rate increases in time. The lower left diagram in Fig. 3 shows the energy transformation ratio indicating that at the end of the process the main fraction of the introduced work is transformed into heat. This behaviour can be explained by the assumed saturated hardening function.

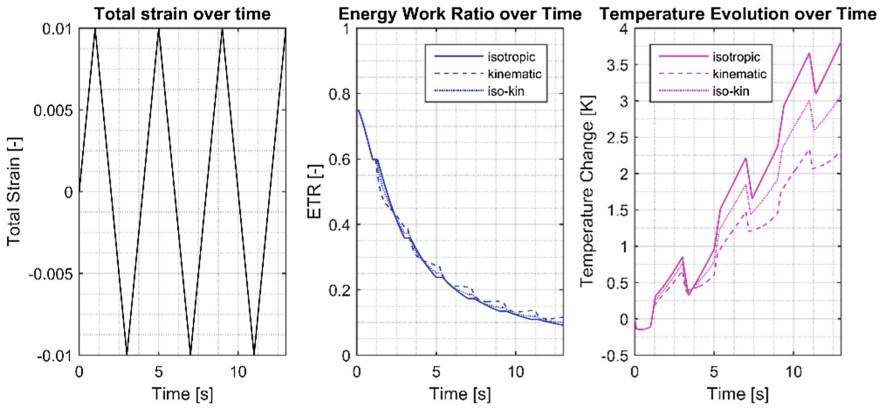

Fig. 4. Parameter variation - different hardening behaviour

Qualitative and quantitative insight is gained due to parametric studies like presented in Fig. 4. A simple strain-controlled experiment (Fig. 4 – left) leads to a significant and measurable temperature difference at the end the load sequence (Fig. 4 – right) while the energy transformation ratio gives only marginal evidence.

5 Summary and Conclusions

This work shows a theoretical framework on the well-known concept of rheological networks to exploit the thermo-mechanical analysis in preparing and evaluating cyclic mechanical test with an additional observation of the temperature field. By proofing a characteristic temperature evolution through a characteristic load cycle sequence experimentally, the validity of the applied material law is confirmed. The presented numerical results meet the temperature range in other publications. Therefore, the parametric studies are going to be extended and the method is going to be transferred to other material classes.

References

1. Chaboche J-L (1989) Constitutive equations for cyclic plasticity and cyclic viscoplasticity. J Plast 3:247–302
2. Haupt, P (2002) Advanced texts in physics. In: Continuum mechanics and theory of materials. 2nd. Berlin Heidelberg: Springer-Verlag
3. Bröcker C, Matzenmiller A (2013) An enhanced concept of rheological models to represent nonlinear thermoviscoplasticity and its energy storage behavior. Cont Mech Therm 25:749–778
4. Yu, Ch, Kang G, Chen K (2017) A hygro-thermo-mechanical coupled cyclic constitutive model for polymers with considering glass transition. Int J Plast 89:29–65

5. Ummenhofer T, Medgenberg J (2006) Numerical modelling of thermoelasticity and plasticity in fatigue-loaded low carbon steels. Quant InfraRed Thermogr J 3(1):71–91. https://doi.org/10.3166/qirt.3.71-91
6. Knysh P, Korkolis YP (2015) Determination of the fraction of plastic work converted into heat in metals. Mech Mater 86:71–80. https://doi.org/10.1016/j.mechmat.2015.03.006